Experiments on Axial Compressive General Instability of Monolithic Ring-Stiffened Cylinders

HERBERT BECKER* AND GEORGE GERARD†
Allied Research Associates, Inc., Concord, Mass.

AND

ROBERT WINTER‡
Avco Corporation, Wilmington, Mass.

Monolithic circumferentially stiffened circular cylindrical shells of moderate length were designed to fail in the axial compressive general instability mode. Detailed discussions of the experiments are presented together with correlation of the results with the predictions of linear theory. The experimental cylinders failed at stresses that averaged 94% of theory. Consequently, it is concluded that linear theory may be used to obtain relatively reliable predictions of compressive general instability stresses in monolithic ring-stiffened circular cylindrical shells for the range of proportions tested.

Nomenclature

A = area of frame, $ab + 0.430\,r^2$, in.^{2}
a = width of frame, in.
b = height of frame, in.
c = total depth of cylinder wall, $t + b$, in.
d = frame spacing, in.
E = Young's modulus
I_f = bending moment of inertia of frame and sheet per unit width, in.^{3}
I_s = bending moment of inertia of stiffener and sheet per unit width, in.^{3}
J = $(J_f + J_s)/2$
J_f = torsional moment of inertia of frame and sheet per unit width, in.^{3}
J_s = torsional moment of inertia of stiffener and sheet per unit width, in.^{3}
k = buckling coefficient
L = length of cylinder, in.
P = axial load, lb
R = centroidal radius of cylinder, in.
r = fillet radius of frame, in.
t = sheet thickness, in.
t_f = area of frame and sheet per unit width, in.
t_s = area of stiffener and sheet per unit width, in.
$\bar{t}$ = effective shear thickness of cylinder wall, in.
U = $k/0.702Z$
Z = dimensionless length parameter
α = $t_s I_f / t_f I_s$
β = wavelength parameter, λ_x/λ_y
$\bar{\beta}$ = $\beta(\bar{t}/t_s)^{1/2}$
γ = $\bar{t}J/4t_f I_s$
λ_x = axial half wavelength of buckle pattern, in.
λ_y = circumferential half wavelength of buckle pattern, in.
ν = Poisson's ratio
σ = axial instability stress, psi

Subscripts

exp = experimental
th = theoretical

Introduction

REFERENCES 1–3 present results obtained during a recent investigation into the general instability characteristics of stiffened circular cylinders. One of the major results of this program was the development of a linear general instability theory for elastic and plastic buckling of orthotropic cylindrical shells under axial compression, external pressure, and torsion over the complete length range.

Since linear theory was employed, it is of particular importance to correlate shell theory with experimental results. Consequently, all available data on stiffened and unstiffened shells were correlated with the theory on a unified basis in Ref. 1. For the lateral pressure case, the experimental results were in good agreement with the predictions of the linear theory. Under torsional loading, the stiffened cylinder data exhibited somewhat more scatter but were in reasonably good agreement with the linear theory to the same extent that the unstiffened cylinder data correlated. Thus, it was concluded that, for lateral pressure and torsion, linear theory provides a satisfactory approach.

For orthotropically stiffened cylinders under axial compression, which is the area of greatest interest in launch and space vehicle applications, there was almost a complete lack of published test data. As a consequence, the experimental program described in this report was conducted on machined orthotropic cylinders of aluminum alloy under axial compression. In all cases, the stiffening system consisted of circumferential rings.

The test data obtained in this program, when compared with the predictions of the linear stability theory, revealed a most significant trend. Most of the test cylinders failed at 85 to 100% of the linear theory, in remarkable contrast with the behavior of isotropic cylinders, which generally fail at 10% of the linear theory for $R/t = 2000$ to 40% of linear theory for $R/t = 100$. Furthermore, the test data on the

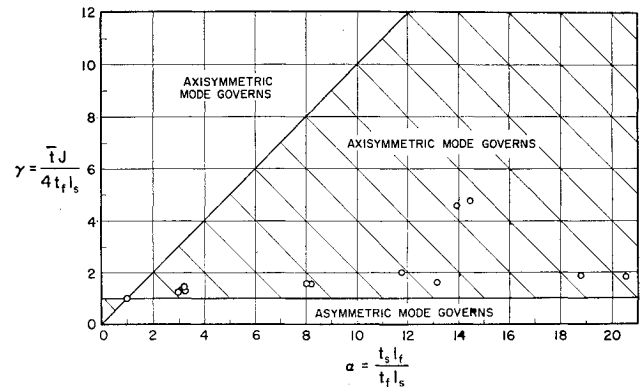

Fig. 1 Experimental cylinders (circles) in $\alpha - \gamma$ domain for moderate length stiffened cylinders

Received December 22, 1962. This work was sponsored by NASA under Research Grant NsG-17-59.

* Chief, Structural Sciences. Member AIAA.

† Director, Engineering Sciences. Associate Fellow Member AIAA.

‡ Associate Scientist, Research and Advanced Development Division. Member AIAA.

circumferentially stiffened cylinders (which were obtained primarily on 8-in.-diam cylinders) exhibited relatively little scatter, particularly as the flexural stiffness in the circumferential direction was increased over that in the longitudinal direction. A corresponding test on a larger diameter cylinder (24 in.) indicated no scale effect.

The theoretical reasons for the behavior of the circumferentially stiffened cylinders advanced in Ref. 3 are related to the fact that such cylinders should buckle first in the axisymmetric mode. Since this mode is stable in the postbuckling region, the deleterious effects of initial imperfections should be minimized, and circumferentially stiffened shells should fail close to the predictions of linear theory.

Instability Characteristics of Moderate-Length Cylinders

Linear orthotropic stability theory yields predictions of the buckling load and buckle mode geometry of an axially compressed ring-stiffened elastic circular cylinder of moderate length. The type of structural performance to be expected from a particular cylinder may be assessed by means of two parameters derived from asymmetric theory which are dependent upon the structural properties of the cylinders. These parameters[1] are

$$\alpha = t_s I_f / t_f I_s \qquad \gamma = \bar{t} J / 4 t_f I_s \tag{1}$$

Using α as the abscissa and γ as the ordinate, the chart of Fig. 1 is obtained which depicts the zones in which various types of instability may be expected in moderate length cylinders.

The buckling parameter of a cylinder is

$$k = 0.702 Z U \tag{2}$$

where

$$\sigma = k\pi^2 E I_s / t_s L^2 \tag{3}$$

$$Z^2 = t_f L^4 / 12 I_s R^2 \tag{4}$$

$$U^2 = (\alpha\bar{\beta}^2 + \gamma)/(\bar{\beta}^2 + 1) \tag{5}$$

$$\bar{\beta}^2 = \beta^2 \bar{t} / t_s \tag{6}$$

Since it is assumed that $\bar{t} = t_s$ in the present program, then $\bar{\beta} = \beta$ and

$$U^2 = (\alpha\beta^2 + \gamma)/(\beta^2 + 1) \tag{7}$$

The wavelength ratio β is a function of α and γ. Details concerning the theoretical calculation of β may be obtained from Ref. 1, Eqs. (30–32). The buckling parameter may be obtained from Eq. (2) only if (α,γ) lies in the real range of Fig. 1. If (α,γ) lies in the imaginary range (i.e., imaginary values of β), then the axisymmetric buckle mode governs the buckle load, and U is equal to 1. More complete discussion of the relationship of the real and imaginary ranges of β and U to values of α and γ appears in Ref. 3.

The relation

$$k = 0.702 Z \tag{8}$$

is the theoretical axisymmetric result. For all cylinders tested in connection with this program β was imaginary, and consequently Eq. (8) applies. This is equivalent to

$$\sigma = 0.577 E (t_s t_f)^{1/2} / R \tag{9}$$

which reduces to the theoretical isotropic result for $\nu = 0$:

$$\sigma = 0.577 E t / R \tag{10}$$

Experimental Procedure

Previous test data on general instability were obtained on cylinders that did not have the structural characteristics of the linear theory with which the test data were compared, as discussed in Refs. 1 and 4. Partially because of this fact, buckling modes other than general instability occurred in those early tests. In order to obtain a valid comparison of orthotropic theory with experimental data, it is necessary that no mode but general instability occur in the cylinder during buckling. For that reason, the present program of experiments on monolithic cylinders was designed and carried out.

In this program the theoretical investigations of Refs. 1 and 2 were used to design cylinders for tests such that no mode but general instability would occur when the cylinders were loaded in axial compression. The details of this selection process are understood best by an examination of the roles played by the various structural parameters pertinent to general instability.

Models and Equipment

Two isotropic and 12 ring-stiffened circular cylinders were loaded to instability in axial compression. The cylinders were nominally 8 and 24 in. in diameter. The program also included an analysis of an experiment performed on a cylinder 7 ft in diameter.[5]

The major variables in the test specimens were the ring spacings, ring details, and shell thicknesses. These are embraced in the two structural parameters, α and γ, which characterize a stiffened cylinder. Table 1 contains the geometric data for all cylinders, whereas the structural parameters appear in Table 2, together with the theoretical and experimental buckling stresses. The sketch on Table 1 depicts the cross-section geometries for the test specimens, all of which buckled elastically in the moderate length range. Young's modulus for all models was 10.6×10^6 psi. The minimum proportional limit stress was 35 ksi, and the yield strength was 44 ksi. This applied to all cylinders, which were 2024-T3 aluminum alloy with the exception of numbers 4 and 10, which were 2014-T6.

In this program, strong emphasis was placed upon the attainment of models of high quality. Because of the uncertainty of dimensional accuracy which was anticipated in the fabrication of a model with separate rings, specimens 3–8 were formed by threading on a lathe. The continuous cutting operation obtained in this fashion was felt to yield a more uniform cylinder wall and rib geometry in the cylinders in which the rib spacings were close enough to permit this procedure.

End Conditions on Cylinders

In order to avoid local buckling at the cylinder ends and uneven circumferential distributions of load, it was important to insure flatness of each end surface. Consequently, all cylinders were fabricated with rings at the ends either integrally machined on the cylinder or cemented to the cylinders after machining. The ends were faced in a lathe to a maximum variation of 0.0005 in. throughout the entire end plane.

In order to observe any possible circumferential variation of axial stress distribution during a test, model 12 was encased in a pair of transparent epoxy rings, which were examined with a polariscope during the test. No significant circumferential variations in photoelastic fringe patterns were observed during the test. Furthermore, the axial loading obtained from the photoelastic data agreed with the load indicated by the testing machine.

Analysis of Data

Effect of Thickness Variation on Instability Stress

The principal datum in each compression test was the axial force P at which failure was observed. However, in order to compare theory and experiment, it is pertinent to examine

Table 1 Geometric data for test cylinders

Specimen no.	R, in.	L, in.	Based on average dimensions: t, 10^{-3} in.	t_f, 10^{-3} in.	I_s, 10^{-7} in.^{3}	I_f, 10^{-7} in.^{3}	J, 10^{-7} in.^{3}	Based on minimum dimensions: t, 10^{-3} in.	t_f, 10^{-3} in.	I_s, 10^{-7} in.^{3}
1	3.80	5.75	7.72	...	...	...	...	7.49	...	...
2	3.73	5.95	9.83	...	...	...	...	9.65	...	...
3	3.81	2.13	19.5	27.4	6.179	26.1	43.5	18.8	25.9	5.54
4	12.23	15.5	34.6	49.0	34.6	152.3	261	33.8	48.6	32.2
5	3.73	5.75	10.6	15.27	0.992	4.59	7.90	10.4	15.1	0.936
6	3.73	1.82	10.4	14.88	0.936	4.34	7.13	10.2	14.7	0.884
7	3.75	3.10	12.3	18.11	1.551	18.44	14.01	11.8	17.6	1.370
8	3.75	1.62	12.2	17.94	1.513	18.37	13.84	11.9	17.6	1.403
9	3.78	4.30	5.01	6.38	0.1050	1.568	1.040	4.66	6.02	0.0844
10[a]	42	48	55.0	69.9	138.7	2320	1061	...	...	...
11	3.74	1.87	10.5	16.15	0.965	21.3	27.3	10.3	15.7	0.910
12	3.74	2.65	10.5	16.25	0.965	21.6	28.2	10.4	16.2	0.936
13	3.74	5.78	12.5	19.40	1.678	49.0	19.40	12.3	19.2	1.551
14	3.74	1.78	12.3	19.12	1.551	49.6	17.83	12.2	19.0	1.513

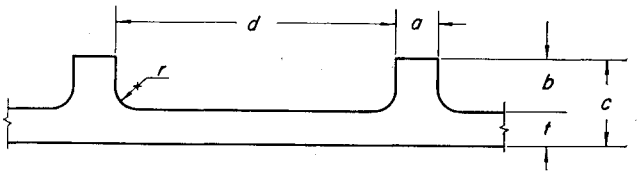

[a] Reference 5.

the ratio $U = \sigma_{exp}/\sigma_{th}$. For a ring-stiffened cylinder, $t_s = t$ and, therefore,

$$\sigma_{exp} = P/2\pi Rt \tag{11}$$

$$\sigma_{th} = 0.577E(tt_f)^{1/2}/R \ (\nu = 0) \tag{12}$$

$$U = P/1.154\pi Et^{3/2}t_f^{1/2} \tag{13}$$

where

$$t_f = (dt + A)/d = t(1 + A/dt) \tag{14}$$

Consequently,

$$U = P/[1.154\pi Et^2(1 + A/dt)^{1/2}] \tag{15}$$

The cylinders that were tested in this program were fabricated with relatively thin walls (t = order of 0.010 in.). Variations in t of the order of several percent were observed throughout each cylinder. This led to some uncertainty as to the proper value to use in Eq. (15), and therefore the test data are presented in terms of both the average measured value of t and the minimum measured value.

Other factors also may be involved, such as the influence of Poisson's ratio and the effect of placing stiffeners on one side of the shell. It was assumed, in deriving Eq. (12), that $\nu = 0$. Actually, it may have a small finite value that would tend to increase σ_{th} and decrease U. One-sided stiffeners, on the other hand, would be expected to decrease σ_{th} and thereby increase U.

Structural Parameters

In plotting k as a function of Z, the position of a test point was determined using the relations

$$Z = (t_f/12I_s)^{1/2}L^2/R \tag{16}$$

$$k = 0.702ZU \tag{17}$$

where U was calculated from Eq. (15). The sensitivity of Z to changes in t is considerably less than the sensitivity of U. For the values of A/dt applicable to the test cylinders of this investigation, $\Delta Z/Z$ was the same order as $\Delta t/t$. This may be seen in Figs. 2 and 3, in which the shift of Z is significantly less than the shift in k for a pair of points at average and minimum dimensions of the test cylinders.

The two structural parameters α and γ are also functions of t. However, in the present study, only the axisymmetric buckle theory was applicable. Consequently, α and γ serve only to characterize the cylinders on the graph of Fig. 1. The precise position of a point on this graph is relatively unimportant. For this reason, only average values of t were used to compute α and γ.

Table 2 Structural parameters and buckling stresses of test cylinders

Specimen no.	α	Based on average dimension: γ	σ_{exp}, ksi	σ_{th}, ksi	U	k_{exp}	Z	Based on minimum dimensions: σ_{exp}, ksi	σ_{th}, ksi	U	k_{exp}	Z	λ_x, in.	λ_y, in.	β	$\left(\frac{t_f}{I_s}\right)^{1/4}\frac{\lambda_x}{R^{1/2}}$
1	1.00	1.00	5.38	12.42	0.433	342	1127	5.54	12.06	0.459	374	1162	...	...	...	...
2	1.00	1.00	10.13	16.17	0.626	424	966	10.32	15.86	0.651	450	985	...	...	...	...
3	3.01	1.25	32.2	37.1	0.869	44.1	72.4	33.3	35.5	0.939	49.0	74.3	0.90	1.95	0.462	6.70
4	3.11	1.33	18.30	20.7	0.885	420	676	18.72	20.3	0.924	452	697	2.50	4.33	0.578	7.80
5	3.21	1.38	18.57	20.9	0.888	627	1007	18.77	20.6	0.910	654	1025	0.62	1.10	0.564	6.38
6	3.24	1.33	18.86	20.5	0.920	66.0	102.2	19.24	20.1	0.957	70.5	104.8	0.62	1.04	0.596	6.40
7	8.07	1.53	23.5	24.4	0.963	171.3	253	24.5	23.6	1.038	193.2	265	0.56	1.30	0.431	5.35
8	8.26	1.56	22.3	24.2	0.920	44.8	69.5	22.9	23.6	0.969	48.8	71.6	0.48	1.88	0.255	4.60
9	11.7	1.95	7.34	9.17	0.801	620	1102	7.89	8.61	0.914	766	1195	...	...	...	...
10[a]	13.2	1.51	7.96	9.03	0.883	696	1123	...	...	...	...	...	3.10	...	...	3.95
11	14.0	4.60	18.40	21.3	0.865	67.0	110.5	18.60	20.8	0.895	70.5	112.2	0.40	1.95	0.205	4.19
12	14.5	4.73	17.82	21.4	0.834	130.8	223	18.03	21.1	0.855	135.0	225	0.40	1.51	0.265	4.20
13	18.8	1.86	23.4	25.8	0.916	565	878	23.8	25.2	0.947	603	907	0.32	1.48	0.216	3.06
14	20.6	1.85	24.5	25.2	0.973	58.6	85.9	24.6	24.9	0.987	60.0	86.7	0.35	1.63	0.215	3.39

[a] Reference 5.

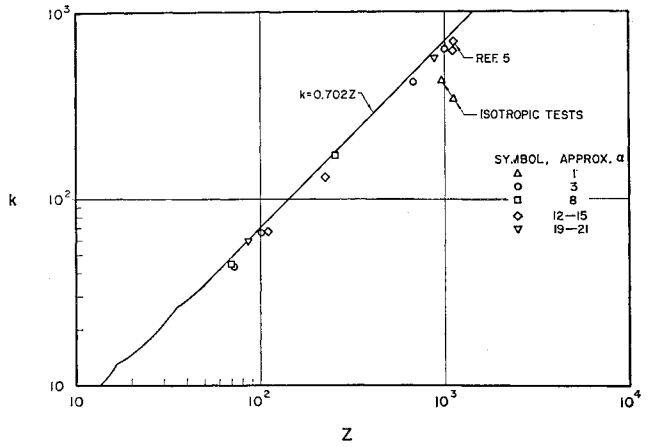

Fig. 2 Comparison of data based on average dimensions with theory of Refs. 1 and 3

The values of I_f were computed from the measured geometric data in the usual manner, as was t_f. For these ring-stiffened cylinders, t_s and $\bar{t}$ were chosen equal to t. The values of J were obtained by the procedure described by Lyse and Johnson.[6]

In addition to the general instability load, records were made of the buckle geometry and the general character of the postbuckling behavior of each cylinder. Numerical data pertaining to the buckles appear in Table 2.

Discussion of Data

General Character of Data

The cylinders investigated in this program failed in general instability with no other buckle mode present, as they were designed to do. All cylinders were in the moderate-length range (Figs. 2 and 3), with a range of α from 1 (isotropic) to 21 and a range of γ from 1.0 to 4.7.

The results are summarized in k-Z form in Figs. 2 and 3, in which the excellent agreement of theory and experiment is evident. The mean value of U based on average dimensions is 0.893, whereas for minimum dimensions it is 0.940. Since local imperfections would be expected to govern the buckling load, it is feasible to regard the minimum dimension data (Fig. 3) as representative of the true structural behavior.

There results indicate that linear theory is satisfactory for predicting reliably the axial load-carrying capacity of the monolithic ring-stiffened circular cylinders tested.

Effect of Imperfections

The effect of initial imperfections would be expected to be strongest at $\alpha = \gamma = 1$, which corresponds to the isotropic

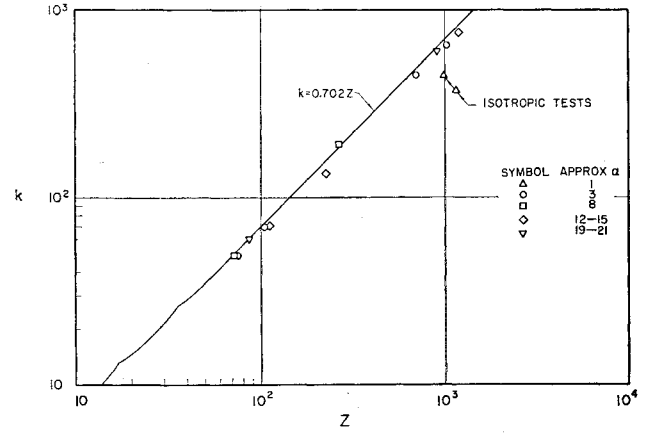

Fig. 3 Comparison of data based on minimum dimensions with theory of Refs. 1 and 3

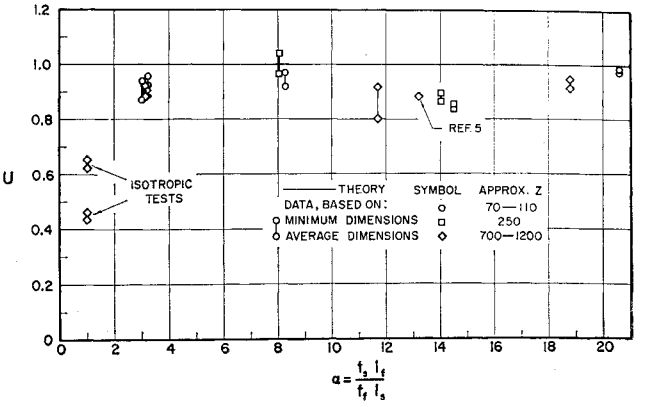

Fig. 4 U vs α for data of Table 2

case, and to diminish with increased α. The test data that are plotted on Fig. 4 show that two isotropic cylinders yielded the expected low value of U, whereas for $\alpha > 3$ the value of U lay essentially within $0.8 < U < 1.0$. Apparently, the transition from U considerably less than 1 to U approaching 1 occurs in the range of $1 \leq \alpha \leq 3$.

Isotropic Tests

Isotropic tests were performed for reference data upon two 8-in. cylinders (see Table 2 for data). Naturally, for these cylinders $\alpha = \gamma = 1$. The results are shown plotted on Fig. 4, which reveals the significant decrease below classical buckling stress to be expected for these two cylinders.

In Table 2, the results are compared to the predictions of σ_{exp} using Fig. 7 of Ref. 7. The experimental data indicate the relatively high quality of fabrication of the models tested in this program.

Buckle Patterns

The buckle patterns observed in the cylinders after test were principally asymmetric, of which a typical result may be seen in Fig. 5. The wavelengths and values of β appear in Table 2.

In some cases, the axisymmetric mode may be that in which buckling originally occurs, after which there is a transition

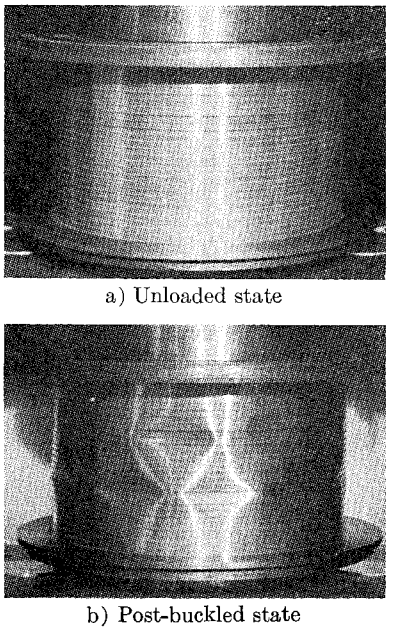

a) Unloaded state

b) Post-buckled state

Fig. 5 Cylinder 9 (α = 12, Z = 1100)

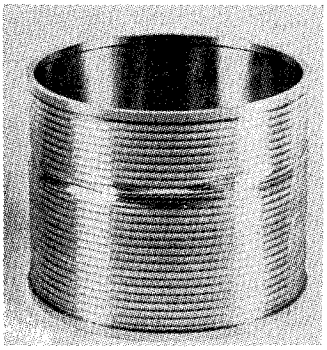

a) Outside view

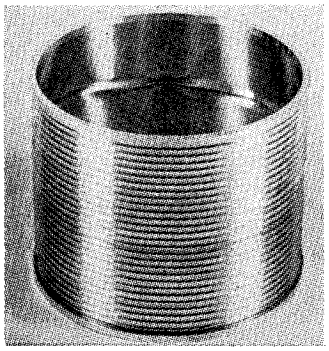

b) Inside view

Fig. 6 Cylinder 13 (α = 19, Z = 878)

to the asymmetric mode as the final form. For imaginary values of β, theoretically the axisymmetric mode is the only mode in which buckling should occur. This applies to all the cylinders investigated in this program. However, because of the speed at which a cylinder usually buckles under axial compression, it may not be possible to observe any buckle mode except the final form, as discussed in Ref. 1.

There was an indication of axisymmetric buckling in four tests (11–14). The final buckle modes for these cylinders appeared to be combinations of axisymmetric and asymmetric patterns, as shown in Fig. 6.

The longitudinal wavelength for axisymmetric general instability may be determined from an expression in Ref. 1 which, in the case of elastic general instability of a ring-stiffened cylinder, may be written in the form

$$(t_f/I_s)^{1/4}\lambda_x/R^{1/2} = \pi \qquad (18)$$

The left-hand side of Eq. (18) was determined from the wavelength measurements made on cylinders with permanent buckles and is plotted in Fig. 7, which reveals a trend of asymmetric data toward the value of π as α increases.

Because of the decrease of buckle wavelength to be anticipated with increased postbuckling and shortening, the left side of Eq. (18) would be expected to be larger for cylinders with buckle stresses considerably below the proportional limit if λ_x is measured immediately after buckling. Consequently the trend of the data in such a case might be similar to that shown in Fig. 7, except that the curve might be higher and tangent to the π line at a different value of α.

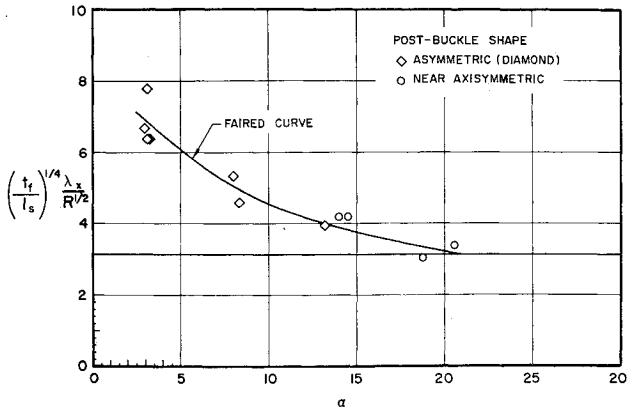

Fig. 7 Axial buckle dimension data compared to theory of Ref. 1, $(t_f/I_s)^{1/4}\lambda_x/R^{1/2} = \pi$

Conclusions

1) The excellent agreement between linear orthotropic theory and experiment obtained for ring-stiffened circular cylindrical shells failing under axial compression in the general instability mode has very significant implications, since it is in direct contrast with the corresponding situation for isotropic cylinders. The small experimental scatter evident in these tests is an important indication of the potential reliability of this type of construction.

2) In view of the good correlation that was obtained for α as low as 3 (the lowest value tested), this tentatively may be selected as the current lower limit of applicability of linear orthotropic theory. The transition from isotropic to orthotropic behavior in the region $1 \leqq \alpha \leqq 3$ requires further investigation.

3) Most of the cylinders of this program were nominally 8 in. in diameter, for which theory agreed well with experiment in the majority of the cases. The test data for the 24-in. and 84-in. cylinders corresponded closely to those for the 8-in. cylinder, and consequently no significant size effect appears to be associated with the circumferentially stiffened cylinders tested.

References

[1] Becker, H. and Gerard, G., "Elastic stability of orthotropic shells," J. Aerospace Sci. **29**, 505–513 (1962).

[2] Gerard, G., "Plastic stability theory of geometrically orthotropic plates and cylindrical shells," J. Aerospace Sci. **29**, 956–962 (1962).

[3] Gerard, G., "Compressive stability of orthotropic cylinders," J. Aerospace Sci. **29**, 1171–1179, 1189 (1962).

[4] Becker, H., "Handbook of structural stability, Part VI: Strength of stiffened curved plates and shells," NACA TN 3786 (July 1958).

[5] Pugliese, P. J., "Tank compression test—model DM-18," Douglas Aircraft Co. Rept. SM-27650 (February 1959).

[6] Lyse, I. and Johnson, B. G., "Structural beams in torsion," Trans. Am. Soc. Civ. Engrs. **101**, 857–896 (1936).

[7] Gerard, G. and Becker, H., "Handbook of structural stability, Part III: Buckling of curved plates and shells," NACA TN 3783 (August 1957).